# $n \rightarrow \pi^*$ Interactions Modulate the Properties of Cysteine Residues and Disulfide Bonds in Proteins



**Citation:** Kilgore, Henry R. and Ronald T. Raines. "n →π* Interactions Modulate the Properties of Cysteine Residues and Disulfide Bonds in Proteins." Journal of the American Chemical Society 140 (2018): 17606-17611 © 2018 The Author(s)

**As Published:** https://dx.doi.org/10.1021/JACS.8B09701

**Publisher:** American Chemical Society (ACS)

**Persistent URL:** https://hdl.handle.net/1721.1/125597

**Version:** Author's final manuscript: final author's manuscript post peer review, without publisher's formatting or copy editing

HHS Public Access

Author manuscript

*J Am Chem Soc*. Author manuscript; available in PMC 2019 May 21.

Published in final edited form as:

*J Am Chem Soc*. 2018 December 19; 140(50): 17606–17611. doi:10.1021/jacs.8b09701.

# $n \rightarrow \pi^*$ Interactions Modulate the Properties of Cysteine Residues and Disulfide Bonds in Proteins

**Henry R. Kilgore** and **Ronald T. Raines**[*]

Department of Chemistry, Massachusetts Institute of Technology, Cambridge, Massachusetts 02139, United States

## Abstract

Noncovalent interactions are ubiquitous in biology, taking on roles that include stabilizing the conformation of and assembling biomolecules, and providing an optimal environment for enzymatic catalysis. Here, we describe a noncovalent interaction that engages the sulfur atoms of cysteine residues and disulfide bonds in proteins—their donation of electron density into an antibonding orbital of proximal amide carbonyl groups. This $n \rightarrow \pi^*$ interaction tunes the reactivity of the CXXC motif, which is the critical feature of thioredoxin and other enzymes involved in redox homeostasis. In particular, an $n \rightarrow \pi^*$ interaction lowers the p$K_a$ value of the N-terminal cysteine residue of the motif, which is the nucleophile that initiates catalysis. In addition, the interplay between disulfide $n \rightarrow \pi^*$ interactions and C5 hydrogen bonds leads to hyperstable β-strands. Finally, $n \rightarrow \pi^*$ interactions stabilize vicinal disulfide bonds, which are naturally diverse in function. These previously unappreciated $n \rightarrow \pi^*$ interactions are strong and underlie the ability of cysteine residues and disulfide bonds to engage in the structure and function of proteins.

## Graphical Abstract

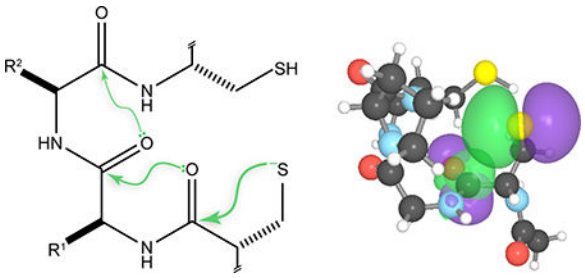


[*]**Corresponding Author** rtraines@mit.edu. Tel: 617-253-1470.

The authors declare no competing financial interest.

ASSOCIATED CONTENT

Supporting Information

The Supporting Information is available free of charge on the ACS Publications website.

Tables S1–S5, S6–S18 (Atomic Coordinates of CXXC Motifs), S19–S24 (Atomic Coordinates of Vicinal Disulfide Bonds), and Figures S1–S3.

## INTRODUCTION

The cysteine residues of proteins have unique attributes. Their sulfhydryl groups not only manifest potent nucleophilicity, but also undergo a facile oxidation reaction to generate disulfide bonds.[1] The descendant cystines are active components of catalytic, oxidation–reduction, and signal transduction pathways,[2] and have distinct physicochemical properties.[3]

Approximately 20% of human proteins are predicted to contain a disulfide bond.[4] Though prevalent, the two sulfur atoms of disulfide bonds are not known to engage with other functional groups in proteins. The unique attributes of disulfide bonds and their component sulfur atoms enticed us to consider their electronic structure in detail.

In a disulfide bond, one lone pair of each sulfur atom resides in a non-degenerate *s*-type orbital ($n_s$; Figure 1A), and the other resides in a non-degenerate *p*-type orbital ($n_p$; Figure 1B).[5] We envisioned that these four lone pairs could interact with nearby carbonyl groups. In particular, donation of lone-pair electron density into the $\pi^*$ orbital of an adjacent carbonyl group could lead to an $n \rightarrow \pi^*$ interaction (Figures 1C and 1D).[6] The shape and higher energy of $n_p$ orbitals confers larger contributions relative to those of $n_s$ orbitals. The existence of such an interaction would underlie an aspect of disulfide bonds that is now unappreciated.

Herein, we use computational methods and bioinformatic analyses to provide evidence that $n \rightarrow \pi^*$ interactions that originate from sulfur play important roles in the structure and function of proteins. The effects arise from the tuning of the thermodynamic stability of the disulfide bonds, thiols, and thiolates of cysteine residues. We find these effects to be especially important in the reactivity of the CXXC motifs in enzymic active sites, interplay with the C5-hydrogen bonds of β-strands, and polarization of electron density in vicinal disulfide bonds.

## RESULTS AND DISCUSSION

Protein structures are stabilized by a web of interplaying noncovalent interactions.[7] This web overpowers entropy only barely, as the free energy difference between the folded and unfolded states is merely 5–15 kcal/mol.[8] We examined three aspects of this web from the perspective of $n \rightarrow \pi^*$ interactions that originate from sulfur.

### Disulfide $n \rightarrow \pi^*$ Interactions within the CXXC Motif

The CXXC motif, in which two cysteine residues are separated by two other residues, is a prevalent feature of enzymes that mediate redox homeostasis.[2c,9] During a catalytic cycle, a disulfide bond is formed and broken between the two cysteine residues of the motif. The sulfhydryl group of a typical cysteine residue has a p$K_a$ value of 8.7.[10] In contrast, the N-terminal cysteine residue in a CXXC motif typically has a p$K_a$ value below physiological pH[12] and is thus highly nucleophilic.[13] The origin of this anomalous acidity has been unclear, despite extensive investigation.[14]

CXXC motifs often reside at the N-terminus of an α-helix. In that context, the sulfur atom ($S_i^{\gamma}$) of only the N-terminal cysteine residue is exposed to solvent. Solvent-accessible

surface area calculations on the crystal structures of oxidized and reduced states of thioredoxin and thioredoxin-2 show that the C-terminal cysteine is completely inaccessible regardless of redox state (Figure S1). Moreover, $S_i^{\gamma}$ of the N-terminal cysteine residue experiences an increase of ~6-fold in solvent-accessible surface area upon reduction of the active-site disulfide bond. Accordingly, we focused our attention on $S_i^{\gamma}$, which is the linchpin of the CXXC motif.

We began by performing Natural Bond Orbital (NBO) second-order perturbation theory calculations on 7 different proteins with an oxidized CXXC motif and a known three-dimensional structure. The results revealed a chain of $n \rightarrow \pi^*$ interactions that stabilize the oxidized state of the CXXC motif (Figure 2A, Table S1). Foremost in this network is the interaction of $S_i^{\gamma}$ and the $C_i{=}O_i$ carbonyl group. Specifically, lone-pair electron density is donated from this sulfur atom into the $\pi^*$ orbital of the carbonyl group, generating a strong $n \rightarrow \pi^*$ interaction in the oxidized, thiol, and thiolate states (Figures 2B–2D; Table S2). The chain is propagated by the formation of a $C_i{=}O_i \cdots C_{i+1}{=}O_{i+1}$ $n \rightarrow \pi^*$ interaction (Figure 2E; Tables S1 and S2), and then a $C_{i+1}{=}O_{i+1} \cdots C_{i+2}{=}O_{i+2}$ $n \rightarrow \pi^*$ interaction (Figure 2F; Tables S1 and S2). This chain of $n \rightarrow \pi^*$ interactions was apparent in all 7 proteins examined and appears to be a ubiquitous feature of CXXC motifs.

Next, we examined oxidized CXXC motifs with known crystal structures and reduction potentials. We found that stronger $n \rightarrow \pi^*$ interactions correlate with lower reduction potentials, that is, more stable disulfide bonds (Figure 3). The effect here is not major, given that 100 mV corresponds to 2.3 kcal/mol.

Nonetheless, the electron-donation that arises from disulfide $n \rightarrow \pi^*$ interactions is likely to increase the electrophilicity of a disulfide bond and thereby enhance its reactivity in thiol–disulfide interchange reactions.

To understand how the chain of $n \rightarrow \pi^*$ interactions within CXXC motifs might be leveraged to perform biochemical functions, we examined well-characterized thioredoxins in more detail. In a CXXC motif, $S_i^{\gamma}$ has three relevant states: disulfide, thiol, and thiolate. Conversion between these states does not induce substantial conformational changes (Figures S1 and S2). The major change incurred upon reduction of the disulfide bond is in the $\chi_1$ dihedral angle (that is, $N_i\text{-}C_i^{\alpha}\text{-}C_i^{\beta}\text{-}S_i^{\gamma}$), which rotates towards the solvent (Figure S2). In the descendant thiol and thiolate, $S_i^{\gamma}$ forms a hydrogen bond with water rather than with $S_{i+3}^{\gamma}$-H or another enzymic functional group. Inspection of both of these three states reveals that all are stabilized by a $S_i^{\gamma} \cdots C_i{=}O_i$ $n \rightarrow \pi^*$ interaction (Figure 4; Tables S1 and S2).

Moreover, the $S_i^{\gamma} \cdots C_i{=}O_i$ $n \rightarrow \pi^*$ interaction tends to be stronger than the $C_i{=}O_i \cdots C_{i+1}{=}O_{i+1}$ or $C_{i+1}{=}O_{i+1} \cdots C_{i+2}{=}O_{i+2}$ interaction. A critical step in catalysis by thioredoxin is deprotonation of $S_i^{\gamma}$ to form the nucleophilic thiolate.[12a] We find that the $S_i^{\gamma} \cdots C_i{=}O_i$ $n \rightarrow \pi^*$ interaction in the thiolate state is much greater than that in the thiol state (Figure 4). This difference is likely to make a significant contribution to the diminished $pK_a$ of the N-terminal cysteine residue in CXXC motifs. The extant explanation for this low thiol $pK_a$ value relies on a presumed macrodipole of the α-helix.[17] The dipole of an α-helix[18] has not

been well-replicated in model systems.[19] Moreover, slightly downstream to many CXXC motifs is a proline residue, which induces a kink in the α-helix.[20] Such a kink would interrupt the projection of the electric field along the helical axis. Notably, calculations of this thiol p$K_a$ have yielded values that are much greater than those observed by experiment,[14,17,21] consistent with $n \rightarrow \pi^*$ interactions being absent from the Hamiltonians employed in typical calculations.

## Interplay of Disulfide $n \rightarrow \pi^*$ Interactions with C5 Hydrogen Bonds

A C5 hydrogen bond is an intrinsic feature of β-strands, arising from the overlap of an $n_p$-type carbonyl lone pair with the $\sigma^*$ orbital of an adjacent amide N–H bond (Figure 5A).[22] Because a large fraction of disulfide bonds in β-strands participate in highly stabilizing $n \rightarrow \pi^*$ interactions, we sought to examine the interplay between a C5 hydrogen bond and a disulfide $n \rightarrow \pi^*$ interaction (Figure 5B). To do so, we examined a disulfide bond that originates from a β-strand (Figure 5C).

A disulfide $n \rightarrow \pi^*$ interaction from $S_i^{\gamma}$ into a carbonyl group polarizes the electron density of the carbonyl group towards its oxygen (Figure 5B). The ensuing increase in electron density could result in a stronger C5 hydrogen bond. We performed relaxed scan calculations of the dihedral angle $\xi$ (that is, $H_i^{\alpha}$–$C_i^{\alpha}$–$N_i$–$H_i$). Each step of these calculations was then subjected to NBO calculations to deconvolute the stabilizing interactions.[23] Specifically, donation of $n_p$ electron density leads to $\Delta E_{n \rightarrow \sigma^*} = 0.30$ kcal/mol at the maximum, an increase of 42% over that in the absence of a $n \rightarrow \pi^*$ interaction. Moreover, the maximal $E_{n \rightarrow \sigma^*}$ is achieved at a dihedral angle $\xi$ that is lower by 15°. In essence, the disulfide $n \rightarrow \pi^*$ interaction increases the polarization of the acceptor carbonyl group, resulting in an increase in the energy of an associated C5 hydrogen bond. This interplay between disulfide bonds and C5 hydrogen bonds bears resemblance to systems in which donation of a hydrogen bond to the oxygen of a carbonyl group enhances the ability of that carbonyl group to accept a stabilizing $n \rightarrow \pi^*$ interaction.[24]

## $n \rightarrow \pi^*$ Interactions of Vicinal Disulfide Bonds

The function of cysteine residues in the proteome spans a vast chemical landscape. Vicinal disulfide bonds constitute an intriguing subset of this landscape.[25] These vicinal disulfide bonds, a sulfur atom is proximal to the carbonyl group of the amide that links the two cysteine residues (Figure 6A). This proximity engenders significant S···C=O $n \rightarrow \pi^*$ interactions (Figure 6B).

The eight-membered ring of a vicinal disulfide bond exists in four distinct conformations (Figures 6C–6F). Each of these conformations entails an $n \rightarrow \pi^*$ interaction. We find that the strongest $n \rightarrow \pi^*$ interactions arise from *trans*-up/down conformations (Figures 6C and 6D), whereas the weakest interactions arise from cis-up conformations (Figures 6E and 6F).

The strong disulfide $n \rightarrow \pi^*$ interactions in *trans*-up/down conformations could play a functional role. These conformations often provide a hydrophobic surface for ligand binding.[2h,25e] Donation of electrons from the $n_s$ and $n_p$ orbitals of a disulfide into the carbonyl $\pi^*$ orbital depletes electron density in the disulfide bond, thereby creating an

electropositive and hydrophobic surface (Figure S3), especially in the *trans*-up/down conformations (Figures S3A and S3B).

## CONCLUSIONS

The role of $n\rightarrow\pi^*$ interactions in protein structure and function became apparent in the early 2000s.[26] Our data expose new terrain in this landscape: the mixing of sulfur $n_s$ and $n_p$ orbitals with proximal carbonyl groups can provide an exceptionally strong $n\rightarrow\pi^*$ interaction that enhances the stability of host secondary structures. In general, the stabilization of oxidized, thiol, or thiolate states through $n\rightarrow\pi^*$ interactions provides a method for fine-tuning vital equilibria in proteins. As cysteine residues are involved in a myriad of biological processes,[2] the contribution of their $n\rightarrow\pi^*$ interactions extends to protein function. In particular, the thermodynamic stability of the CXXC motif, which is the centerpiece of redox homoeostasis, is underpinned by $n\rightarrow\pi^*$ interactions. Finally, we note that the enhanced ability of selenium to donate an $n\rightarrow\pi^*$ interaction[29] suggests that the effects that we observe with cysteine residues could be amplified with selenocysteine.[30]

## EXPERIMENTAL METHODS

### Calculations

All quantum mechanical calculations were performed with Gaussian 09, revision E.01[31] at the M062x/6–311+g(2d,p) level of theory. Energies (*i.e.*, $E_{n\rightarrow\pi^*}$ and $E_{n\rightarrow\sigma^*}$) were calculated by second-order perturbation theory analysis of optimized structures as implemented with NBO 6.0[32] in Gaussian 09, revision E.01.[31] Images of orbitals were generated with the program NBOView 1.1.[33]

The atomic coordinates of CXXC motifs were extracted from the PDB files of parent enzymes. The $C^{\alpha}$ atoms (and thus the side chains) were fixed while other main-chain atoms were allowed to optimize. Optimized structures were consistent with those from molecular dynamics and QM/MM calculations.[21,34]

One-dimensional scan calculations were performed by increasing the dihedral angle $\xi$ in 10°-steps and allowing the structure to optimize.

## Supplementary Material

Refer to Web version on PubMed Central for supplementary material.

## ACKNOWLEDGMENT

We thank Dr. Emily R. Garnett for pointing us toward the disulfide bonds of human chorionic gonadotropin.

Funding Sources

This work was supported by Grant R01 GM044783 (NIH).

## ABBREVIATIONS

| | |
|---|---|
| **CXXC** | Cys-Xaa-Xaa-Cys (where “Xaa” refers to any amino-acid residue) |

| | |
|---|---|
| **NBO** | Natural Bond Orbital |
| **PDB** | Protein Data Bank |

## REFERENCES


(1). Poole LB The basics of thiols and cysteines in redox biology and chemistry. Free Radic. Biol. Med 2015, 80, 148–157. [PubMed: 25433365]

(2) (a). Wall JS Disulfide bonds: Determination, location, and influence on molecular properties of proteins. J. Agr. Food Chem 1971, 19, 619–625. [PubMed: 5163841] (b)Benham CJ; Jafri MS Disulfide bonding patterns and protein topologies. Protein Sci. 1993, 1, 41–54.(c)Chivers PT; Prehoda KE; Raines RT The CXXC motif: A rheostat in the active site. Biochemistry 1997, 36, 4061–4066. [PubMed: 9099998] (d)Woycechowsky KJ; Raines RT Native disulfide bond formation in proteins. Curr. Opin. Chem. Biol 2000, 4, 533–539. [PubMed: 11006541] (e)Schmidt B; Ho L; Hogg PJ Allosteric disulfide bonds. Biochemistry 2006, 45, 7429–7433. [PubMed: 16768438] (f)Pace NJ; Weerapana E Diverse functional roles of reactive cysteines. ACS Chem. Biol 2013, 8, 283–296. [PubMed: 23163700] (g)Góngora-Benítez M; Tulla-Puche J; Albericio F Mutlifacted roles of disulfide bonds: Peptides as therapeutics. Chem. Rev 2013, 114, 901–926. [PubMed: 24446748] (h)Paulsen CE; Carroll KS Cysteine-mediated redox signaling: Chemistry, biology and tools for discovery. Chem. Rev 2013, 113, 4633–4679. [PubMed: 23514336] (i)Go Y-M; Jones DP The redox proteome. J. Biol. Chem 2013, 288, 26512–26520. [PubMed: 23861437] (j)Skryhan K; Cuesta-Siejo JA; Nielsen MM; Marri L; Mellor SB; Glaring MA; Jensen PE; Palcic MM; Blennow A The role of cysteine residues in redox regulation and protein stability of *Arabidopsis thaliana* starch synthase 1. PLoS ONE 2015, 10, e0136997. [PubMed: 26367870] (k)Majmudar JD; Konopko AM; Labby KJ; Tom CT; Crellin JE; Prakash A; Martin BR Harnessing redox cross-reactivity to profile distinct cysteine modifications. J. Am. Chem. Soc 2016, 136, 1852–1859.(l)Manteca A; Alonso-Caballero Á; Fertin M; Poly S; De Sancho D; Perez-Jimenez R The influence of disulfide bonds on the mechanical stability of proteins is context dependent. J. Biol. Chem 2017, 292, 13374–13380. [PubMed: 28642368]

(3) (a). Burns JA; Whitesides GM Predicting the stability of cyclic disulfides by molecular modeling: “Effective Concentrations” in thiol–disulfide interchange and the design of strongly reducing dithiols. J. Am. Chem. Soc 1990, 112, 6296–6303.(b)Klink TA; Woycechowsky KJ; Taylor KM; Raines RT Contribution of disulfide bonds to the conformational stability and catalytic activity of ribonuclease A. Eur. J. Biochem 2000, 267, 566–572. [PubMed: 10632727] (c)Kucharski TJ; Huang Z; Yang Q-Z; Tian Y; Rubin NC; Concepcion CD; Boulatove R Kinetics of thiol/disulfide exchange correlate weakly with the restoring force in the disulfide moiety. Angew. Chem., Int. Ed 2009, 48, 7040–7043.(d)Dopieralski P; Ribas-Arino J; Anjukandi P; Krupicka M; Kiss J; Marx D The Janus-faced role of external forces in the mechanochemical disulfide bond cleavage. Nat. Chem 2013, 5, 685–691. [PubMed: 23881500]

(4). Martelli PL; Fariselli P; Casadio R Prediction of disulfide-bonded cysteines in proteomes with a hidden neural network. Proteomics 2004, 4, 1665–1671. [PubMed: 15174135]

(5). Clauss AD; Nelsen SF; Ayoub M; Moore JW; Landis CR; Weinhold F Rabbit-ears hybrids, VSEPR sterics, and other orbital anachronisms. Chem. Educ. Res. Pract 2014, 15, 417–434.

(6). Newberry RW; Raines RT The $n \rightarrow \pi^*$ interaction. Acc. Chem. Res 2017, 50, 1838–1846. [PubMed: 28735540]

(7) (a). Riley KE; Pitoňák M; Jurečka P; Hobza P Stabilization and structure calculations for noncovalent interactions in extended molecular systems based on wave function and density functional theories. Chem. Rev 2010, 110, 5023–5063. [PubMed: 20486691] (b)Scheiner S, Ed. Noncovalent Forces. Springer: Cham, Switzerland, 2015.

(8) (a). Dill KA Dominant forces in protein folding. Biochemistry 1990, 29, 7133–7155. [PubMed: 2207096] (b)Richards FM Protein stability: Still an unsolved problem. Cell. Mol. Life Sci 1997, 53, 790–802. [PubMed: 9413550]

(9) (a). Kadokura H; Katzen F; Beckwith J Protein disulfide bond formation in prokaryotes. Annu. Rev. Biochem 2003, 72, 111–135. [PubMed: 12524212] (b)Sollioz M; Stoyanov JV Copper homeostasis in Eterococcus hirae. FEMS Microbiol. Rev 2003, 27, 183–195. [PubMed:

12829267] (c)Formenko DE; Gladyshev VN Identity and functions of CXXC-derived motifs. Biochemistry 2003, 24, 11214–11225.(d)Tu BP; Weissman JS Oxidative protein folding in eukaryotes: Mechanisms and consequences. J. Cell Biol 2004, 164, 341–346. [PubMed: 14757749] (e)Lopez-Mirabal HR; Winther JR Redox characteristics of the eukaryotic cytosol. Biochim. Biophys. Acta 2008, 1783, 629–640. [PubMed: 18039473]

(10). Szajewski RP; Whitesides GM Rate constants and equilibrium constants for thiol–disulfide interchange reactions involving oxidized glutathione. J. Am. Chem. Soc 1978, 102, 2011–2026.

(11). Weichsel A; Gasdaska JR; Powis G; Montfort WR Crystal structures of reduced, oxidized, and mutated human thioredoxins: Evidence for a regulatory homodimer. Structure 1996, 4, 735–751. [PubMed: 8805557]

(12) (a). Chivers PT; Prehoda KE; Volkman BF; Kim BM; Markley JL; Raines RT Microscopic p$K_a$ values of *Escherichia coli* thioredoxin. Biochemistry 1997, 36, 14985–14995. [PubMed: 9398223] (b)Kersteen EA; Raines RT Catalysis of disulfide bond formation by protein disulfide isomerase and small-molecule mimics. Antioxid. Redox Signal 2003, 5, 413–424. [PubMed: 13678529]

(13). Bednar RA Reactivity and pH dependence of thiol conjugation to *N*-ethylmaleimide: Detection of a conformational change in chalcone isomerase. Biochemistry 1990, 29, 3684–3690. [PubMed: 2340265]

(14). Cheng Z; Jinfeng Z; Ballou DP; Williams CH Reactivity of thioredoxin as a protein thiol–disulfide oxidoreductase. Chem. Rev 2011, 111, 5768–5783. [PubMed: 21793530]

(15). Guddat LW; Bardwell JC; Martin JL Crystal structures of reduced and oxidized DsbA: Investigation of domain motion and thiolate stabilization. Structure 1998, 6, 757–767. [PubMed: 9655827]

(16). Roos G; Garcia-Pino A; Van belle K; Brossens E; Wahni K; Vandenbussche G; Wyns L; Loris R; Messens J The conserved active site proline determines the reducing power of *Staphylococcus aureus* thioredoxin. J. Mol. Biol 2007, 368, 800–811. [PubMed: 17368484]

(17). Roos G; Foloppe N; Messens J Understanding the pKa of redox cysteines: The key role of hydrogen bonding. Antiox. Redox Signal 2013, 18, 94–127.

(18) (a). Hol WGJ; van Duijnen PT; Berendsen HJC The α-helix dipole and the properties of proteins. Nature 1978, 273, 443–446. [PubMed: 661956] (b)Creighton TE Proteins: Structures and Molecular Properties, 2nd *ed* W. H. Freeman: New York, NY, 1993, pp 183–186 and 335–336.

(19) (a). Huyghues-Despointes BMP; Scholtz JM; Baldwin RL Effect of a single aspartate on helix stability at different positions in neutral alanine-based peptide. Protein Sci. 1993, 2, 1604–1611. [PubMed: 8251935] (b)Armstrong KM; Baldwin RL Charged histidine affects α-helix stability at all positions by interacting with the backbone charges. Proc. Natl. Acad. Sci. USA 1993, 90, 11337–11340. [PubMed: 8248249] (c)Joshi HV; Meier M The effect of a peptide helix macrodipole moment on the p$K_a$ of an Asp side chain carboxylate. J. Am. Chem. Soc 1996, 118, 12038–12044.

(20). Eklund H; Gleason FK; Holmgren A Structural and Functional relations among thioredoxins of different species. Proteins: Struct. Funct. Genet 1991, 11, 13–28. [PubMed: 1961698]

(21). Karshikoff A; Nilsson L; Foloppe N Understanding the −C−X1−X2−C− motif in the active site of the thioredoxin superfamily: *E. coli* DsbA and its mutants as a model system. Biochemistry 2013, 52, 5730–5745. [PubMed: 23879632]

(22). Newberry RW; Raines RT A prevalent intraresidue hydrogen bond stabilizes proteins. Nat. Chem. Bio 2016, 12, 1084–1085. [PubMed: 27748749]

(23)(a). Weinhold F; Landis CR Discovering Chemistry with Natural Bond Orbitals. John Wiley & Sons: Hoboken, NJ, 2012.(b)Weinhold F Natural bond orbital analysis: A critical overview of relationships to alternative bonding perspectives. J. Comput. Chem 2012, 33, 2363–2379. [PubMed: 22837029]

(24) (a). Kuemin M; Nagel YA; Schweizer S; Monnard FW; Ochsenfeld C; Wennemers H Tuning the *cis*/*trans* conformer ratio of Xaa–Pro amide bonds by intramolecular hydrogen bonds: The effect on PPII helix stability. Angew. Chem., Int. Ed 2010, 49, 6324–6327.(b)Shoulders MD; Kotch FW; Choudhary A; Guzei IA; Raines RT The aberrance of the 4*S* diastereomer of 4-hydroxyproline. J. Am. Chem. Soc 2010, 132, 10857–10865. [PubMed: 20681719] (c)Erdmann RS; Wennemers H Effect of sterically demanding substituents on the conformational stability of

the collagen triple helix. J. Am. Chem. Soc 2012, 134, 17117–17124. [PubMed: 22992124] (d)Siebler C; Erdmann RS; Wennemers H Switchable proline derivatives: Tuning the conformational stability of the collagen triple helix by pH changes. Angew. Chem., Int. Ed 2014, 53, 10340–10344.(e)Siebler C; Trapp N; Wennemers H Crystal structure of (4S)-aminoproline: Conformational insight into a pH-responsive proline derivative. J. Pept. Sci 2015, 21, 208–211. [PubMed: 25581874]

(25) (a). Xia Z-X; Dai W.-w.; Zhang Y.-f.; White SA; Boyd GD; Mathews SF Determination of the gene sequence and the three-dimensional structure at 2.4 Å resolution of methanol dehydrogenase from *Methylophilus* W3A1. J. Mol. Biol 1996, 259, 480–501. [PubMed: 8676383] (b)Kim B-M; Schultz LW; Raines RT Variants of ribonuclease inhibitor that resist oxidation. Protein Sci. 1999, 8, 430–434. [PubMed: 10048337] (c) Park C; Raines RT Adjacent cysteine residues as a redox switch. Protein Eng. 2001, 14, 939–942. [PubMed: 11742114] (d)Ledwidge R; Patel B; Dong A; Fiedler D; Falkowski M; Zelikova J; Summers AO; Pai EF; Miller SM NmerA, the metal binding domain of mercuric ion reductase, removes $Hg^{2+}$ from proteins, delivers it to the catalytic core, and protects cells under glutathione-depleted conditions. Biochemistry 2005, 44, 11402–11416. [PubMed: 16114877] (e)Richardson JS; Videau LL; Williams CJ; Richardson DC Broad analysis of vicinal disulfides: Occurrences, conformations with *cis* or with *trans* peptides, and functional roles including sugar binding. J. Mol. Biol 2017, 429, 1321–1335. [PubMed: 28336403]

(26) (a). Bretscher LE; Jenkins CL; Taylor KM; DeRider ML; Raines RT Conformational stability of collagen relies on a stereoelectronic effect. J. Am. Chem. Soc 2001, 123, 777–778. [PubMed: 11456609] (b)Hinderaker MP; Raines RT An electronic effect on protein structure. Protein Sci. 2003, 12, 1188–1194. [PubMed: 12761389] (c)Choudhary A; Gandla D; Krow GR; Raines RT Nature of amide carbonyl–carbonyl interactions in proteins. J. Am. Chem. Soc 2009, 131, 7244–7246. [PubMed: 19469574] (d)Bartlett GJ; Choudhary A; Raines RT; Woolfson DN $n \rightarrow \pi^*$ Interactions in proteins. Nat. Chem. Biol 2010, 6, 615–620. [PubMed: 20622857]

(27). Miyanaga A; Koseki T; Matsuzawa H; Wakagi T; Shoun H; Fushinobu S Crystal structure of a family 54 α-L-arabinofuranosidase reveals a novel carbohydrate-binding module that can bind arabinose. J. Biol. Chem 2004, 279, 44907–44914. [PubMed: 15292273]

(28). Alhassid A; Ben-David A; Tabachnikov O; Libster D; Naveh E; Zolotnitsky G; Shoham Y; Shoham G Crystal structure of an inverting GH 43 1,5-α-L-arabinanase from *Geobacillus stearothermophilus* complexed with its substrate. Biochem. J 2009, 422, 73–82. [PubMed: 19505290]

(29). Guzei IA; Choudhary A; Raines RT Pyramidalization of a carbonyl C atom in (2S)-N-(selenoacetyl)proline methyl ester. Acta Crystallogr. 2013, E69, o805–o806.

(30). Reich HJ; Hondal RJ Why Nature chose selenium. ACS Chem. Biol 2016, 11, 821–841. [PubMed: 26949981]

(31). Frisch MJ; Trucks GW; Schlegel HB; Scuseria GE; Robb MA; Cheeseman JR; Scalmani G; Barone V; Petersson GA; Nakatsuji H; Li X; Caricato M; Marenich A; Bloino J; Janesko BG; Gomperts R; Mennucci B; Hratchian HP; Ortiz JV; Izmaylov AF; Sonnenberg JL; Williams-Young D; Ding F; Lipparini F; Egidi F; Goings J; Peng B; Petrone A; Henderson T; Ranasinghe D; Zakrzewski VG; Gao J; Rega N; Zheng G; Liang W; Hada M; Ehara M; Toyota K; Fukuda R; Hasegawa J; Ishida M; Nakajima T; Honda Y; Kitao O; Nakai H; Vreven T; Throssell K; Montgomery JA Jr.; Peralta JE; Ogliaro F; Bearpark M; Heyd JJ; Brothers E; Kudin KN; Staroverov VN; Keith T; Kobayashi R; Normand J; Raghavachari K; Rendell A; Burant JC; Iyengar SS; Tomasi J; Cossi M; Millam JM; Klene M; Adamo C; Cammi R; Ochterski JW; Martin RL; Morokuma K; Farkas O; Foresman JB; Fox DJ Gaussian 09, Revision E.01, Gaussian, Inc.: Wallingford, CT, 2016.

(32). Glendening ED; Badenhoop JK; Reed AE; Carpenter JE; Bohmann JA; Morales CM; Landis CR; Weinhold F NBO 6.0, Theoretical Chemistry Institute, University of Wisconsin–Madison: Madison, WI, 2013.

(33). Wendt M; Weinhold F NBOView 1.1, Theoretical Chemistry Institute, University of Wisconsin–Madison: Madison, WI, 2001.

(34). Rickard GA; Berges J; Houee-Levin C; Rauk A *Ab initio* QM/MM study of electron addition on the disulfide bond in thioredoxin. J. Phys. Chem. B 2008, 112, 5774–5787. [PubMed: 18447348]

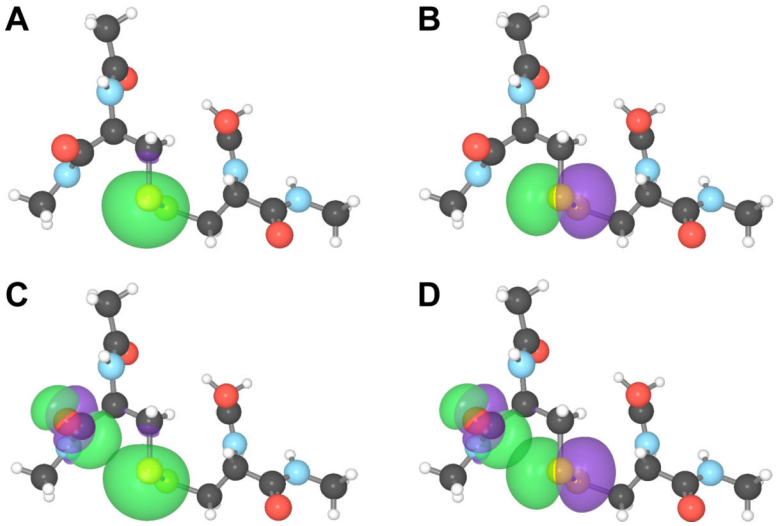


**Figure 1.**

Images of the sulfur lone pairs in *N*-acetyl-cysteine methyl amide disulfide with surrounding carbonyl groups. (A) Sulfur lone pair in the $n_s$ orbital. (B) Sulfur lone pair in the $n_p$ orbital. (C) $n_s^{\gamma} \rightarrow \pi^*$ interaction between $S_i^{\gamma}$ and $C_i{=}O_i$. (D) $n_p^{\gamma} \rightarrow \pi^*$ interaction between $S_i^{\gamma}$ and $C_i{=}O_i$.

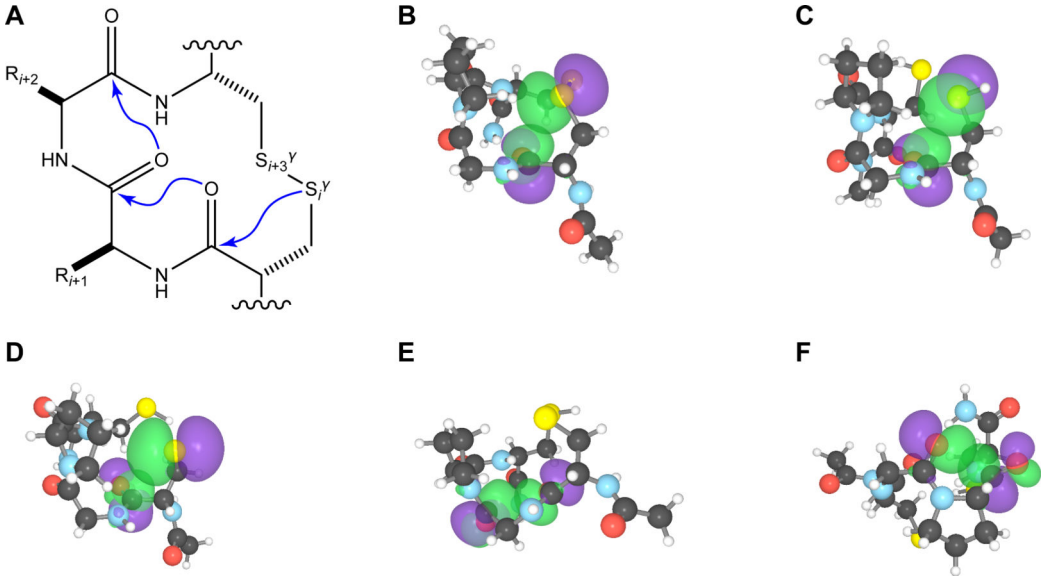


**Figure 2.**

Network of $n \rightarrow \pi^*$ interactions within the CXXC motif. (A) Electron donation in the oxidized state. (B) $S_i^{\gamma} \cdots C_i{=}O_i$ $n \rightarrow \pi^*$ interaction in the oxidized state. (C) $S_i^{\gamma} \cdots C_i{=}O_i$ $n \rightarrow \pi^*$ interaction in the thiol state. (D) $S_i^{\gamma} \cdots C_i{=}O_i$ $n \rightarrow \pi^*$ interaction in the thiolate state. (E) $C_i{=}O_i \cdots C_{i+1}{=}O_{i+1}$ $n \rightarrow \pi^*$ interaction in the thiolate state. (F) $C_{i+1}{=}O_{i+1} \cdots C_{i+2}{=}O_{i+2}$ $n \rightarrow \pi^*$ interaction in the thiolate state. Structures are from PDB entries 1ert and 1eru.[11]

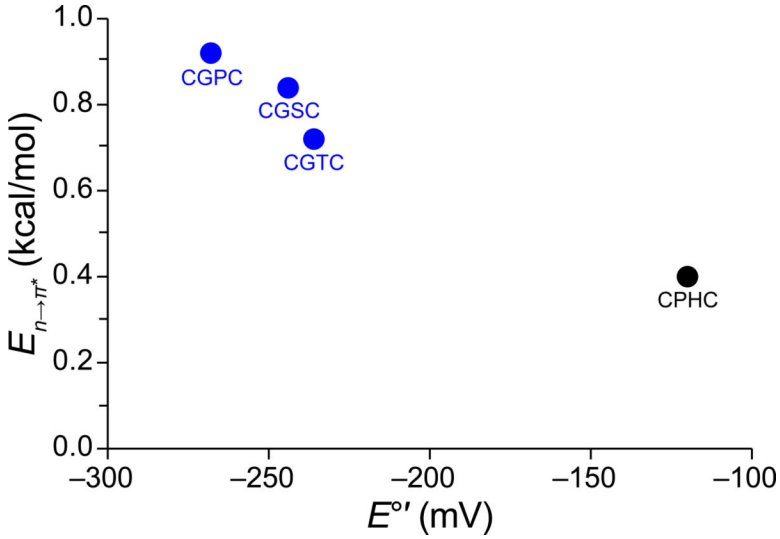


**Figure 3.**

Graph of the relationship between calculated $E_{n\rightarrow\pi^*}$ values and measured $E°'$ values for CXXC motifs: *Escherichia coli* DsbA (black; PDB entry 1a2j[15]) and three variants of *Staphylococcus aureus* thioredoxin (blue; PDB entries 2o7k, 2o85, and 2o87[16]).

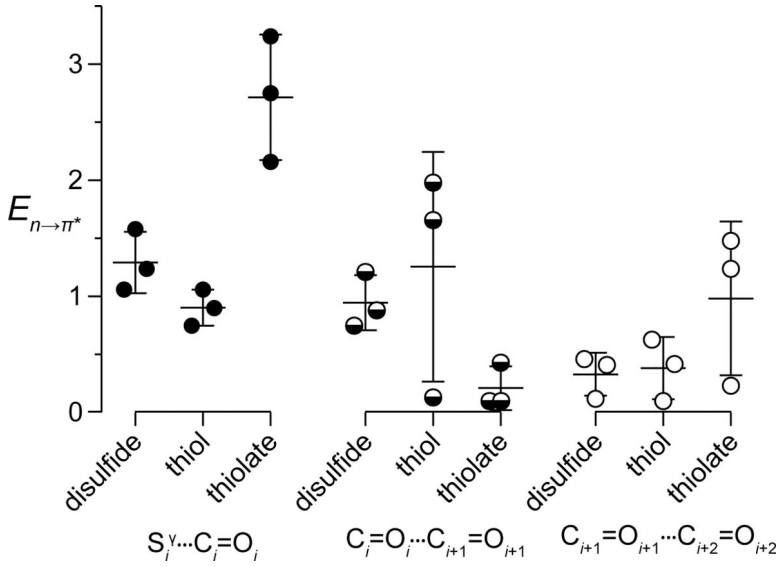


**Figure 4.**

Graph showing calculated $E_{n\rightarrow\pi^*}$ values (in kcal/mol) within the CXXC motifs of *Homo sapiens* thioredoxin and thioredoxin-2, and *Drosophila melanogaster* thioredoxin. Data are listed in Table S2.

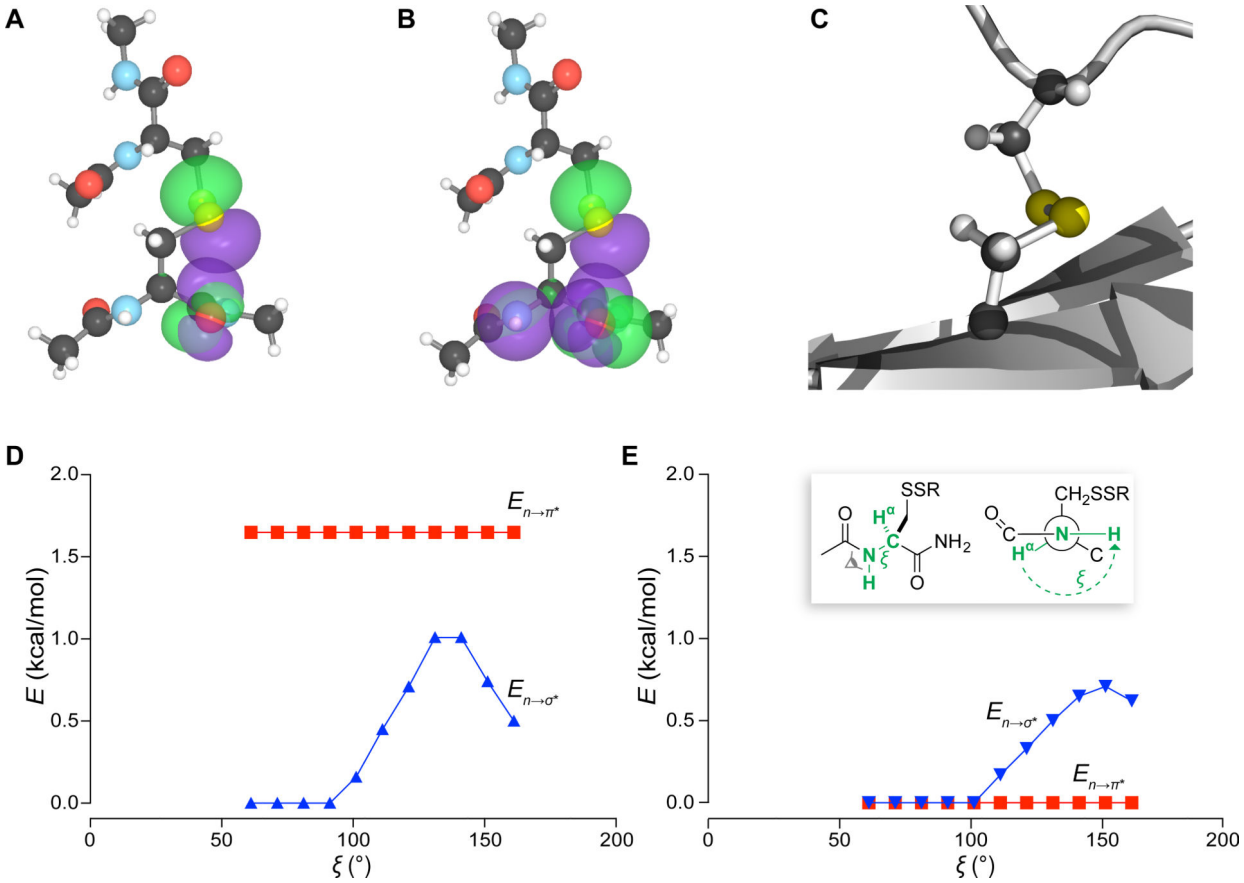


**Figure 5.**

Interplay between a disulfide $n\to\pi^*$ interaction and C5 hydrogen bond in a β-strand. (A) Natural bond orbitals showing a disulfide $n\to\pi^*$ interaction. (B) Network of natural bond orbitals in which the $n\to\pi^*$ interaction from panel A enhances an $n\to\sigma^*$ interaction (that is, a C5 hydrogen bond) within the half-cystine residue. (C) Image of a model disulfide bond. (D) Scan of the dihedral angle $\xi$ (which is defined in the inset of panel E) in the presence of a disulfide $n\to\pi^*$ interaction of $E_{n\to\pi^*}$ = 1.65 kcal/mol; data are listed in Table S3. (E) Scan of the dihedral angle $\xi$ in the absence of a disulfide $n\to\pi^*$ interaction; data are listed in Table S4. The structure in panels A–C is from PDB entry 4gn2 (Table S5) and was used in the calculations of panels D and E.

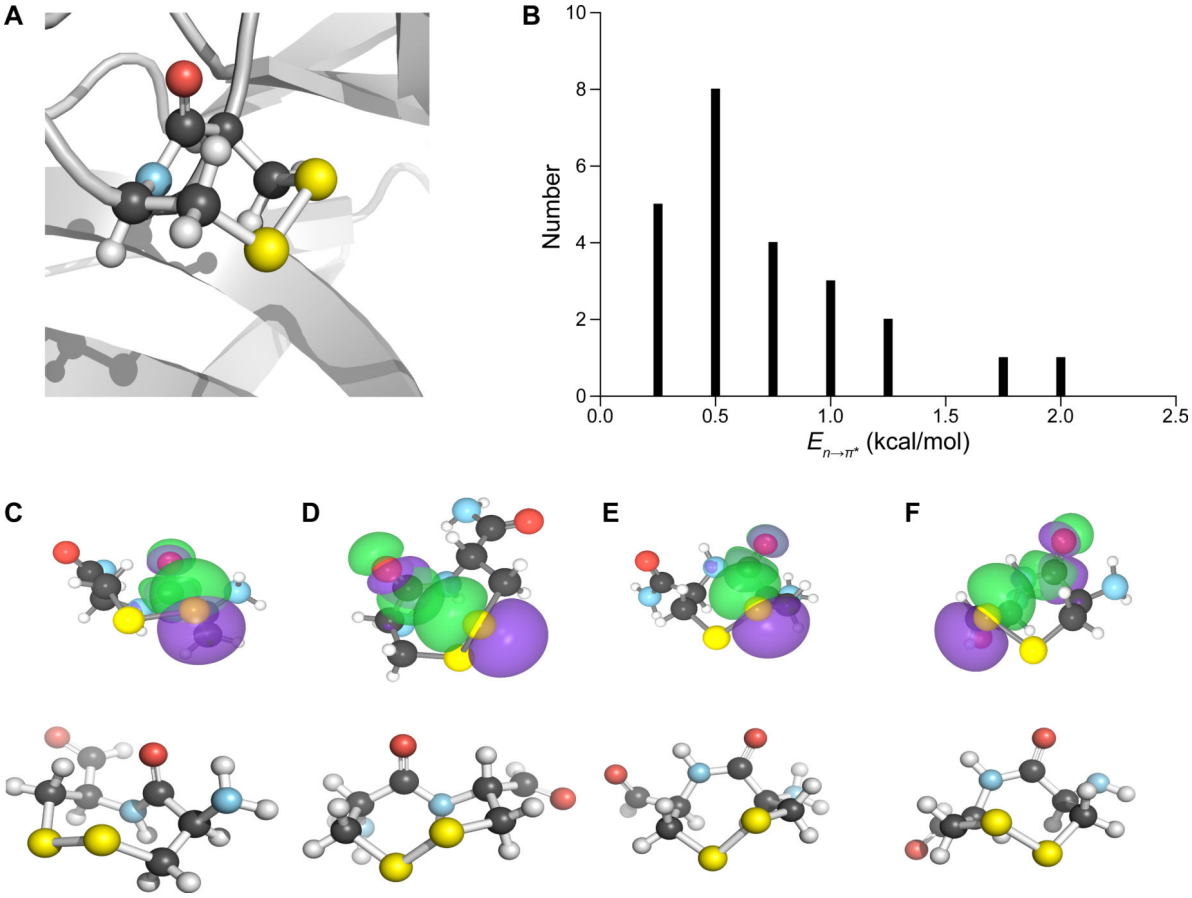


**Figure 6.**

$n\rightarrow\pi^*$ Interactions of vicinal disulfide bonds. (A) Image of a model vicinal disulfide bond (PDB entry 3cu9[27]). (B) Histograms of $n\rightarrow\pi^*$ interaction energies of vicinal disulfide bonds in protein crystal structures. Twenty-four vicinal disulfide bonds from the PDB were subjected to NBO analysis, and the resulting $E_{n\rightarrow\pi^*}$ values were put into bins of 0.25 kcal/mol. (C–F) Natural bond orbitals for the strongest disulfide $n\rightarrow\pi^*$ interaction in the four conformations of vicinal disulfide bonds: *trans*-up conformation (panel C; 3cu9[27]), *trans*-down conformation (panel D; 4aah[25a]), *cis*-up conformation (panel E; 1wd3[28]), and *cis*-down conformation (panel F; 4mge).